Reisbig, R. R., & Hearst, J. E. (1981) *Biochemistry 20*, 1907-1918.
Reisler, E., & Eisenberg, H. (1969) *Biochemistry 8*, 4572-4576.
Richey, B., Cayley, D. S., Mossing, M. C., Kolka, C., Anderson, C. F., Farrar, T. C., & Record, M. T., Jr. (1987) *J. Biol. Chem. 262*, 7157-7164.
Schachman, H. K. (1959) *Ultracentrifugation in Biochemistry*, Academic Press, New York.
Seifried, S. E., Wang, Y., & von Hippel, P. H. (1988) *J. Biol. Chem. 263*, 13511-13514.
Seifried, S. E., Bjornson, K. P., & von Hippel, P. H. (1991) *J. Mol. Biol. 211*, 1139-1151.
Sharp, J. A., & Platt, T. (1984) *J. Biol. Chem. 259*, 2268-2273.
Stockel, P., May, R., Strett, I., Zdenka, C., Hoppe, W., Heumann, H., Zillig, W., Crespi, H. L., Katz, J. J., & Ibel, K. (1979) *J. Appl. Crystallogr. 12*, 176.
Van Holde, K. E. (1967) *Fractions*, Vol. 1, pp 1-10, Spinco Division, Beckman Instruments, Palo Alto, CA.
Van Holde, K. E. (1975) in *The Proteins* (Neurath, H., & Hill, R. L., Eds.) 3rd, ed., Vol. 1, pp 225-291, Academic Press, New York.
Van Holde, K. E., & Weischet, W. O. (1978) *Biopolymers 17*, 1387-1403.
von Hippel, P. H., Bear, D. G., Morgan, W. D., & McSwiggen, J. A. (1984) *Annu. Rev. Biochem. 53*, 389-446.
Weast, R. C. (1978) *Handbook of Chemistry and Physics*, CRC Press, Cleveland, OH.
Yager, T. D., & von Hippel, P. H. (1987) in *E. coli and S. typhimurium: Cellular and Molecular Biology* (Neidhardt, F. C., Ingraham, J. L., Low, K. B., Magasanik, B., Schaechter, M., & Umbarger, H. E., Eds.) pp 1241-1275, American Society for Microbiology, Washington, DC.

Physical Properties of the *Escherichia coli* Transcription Termination Factor Rho. 2. Quaternary Structure of the Rho Hexamer†

Johannes Geiselmann,‡ Steven E. Seifried, Thomas D. Yager,§ Cheryl Liang,‖ and Peter H. von Hippel*
Institute of Molecular Biology and Department of Chemistry, University of Oregon, Eugene, Oregon 97403
Received May 13, 1991; Revised Manuscript Received August 22, 1991

ABSTRACT: Under approximately physiological conditions, the transcription termination factor rho from *Escherichia coli* is a hexamer of planar hexagonal geometry [Geiselmann, J., Yager, T. D., Gill, S. C., Calmettes, P., & von Hippel, P. H. (1992) *Biochemistry* (preceding paper in this issue)]. Here we describe studies that further define the quaternary structure of this hexamer. We use a combination of chemical cross-linking and treatment with mild denaturants to show that the fundamental unit within the rho hexamer is a dimer stabilized by an isologous (or pseudoisologous) bonding interface. Three identical dimers of rho interact via a second type of isologous bonding interface to yield a hexamer with C_3 or D_3 symmetry. Cross-linking and denaturation experiments definitely rule out C_6 and C_2 symmetry for the rho hexamer. Data from fluorescence quenching, lifetime, and energy transfer experiments also argue against C_2 symmetry. The *simplest* symmetry assignment that is not contradicted by any experimental data is D_3; thus we conclude that the rho hexamer has D_3 symmetry. We also consider the positioning of the binding sites for RNA and ATP relative to the coordinate reference frame of the D_3 hexamer. Fluorescence energy transfer data are presented and integrated with data from the literature to arrive at a self-consistent model for the quaternary structure of the rho hexamer.

The quaternary structure of a protein must be known before its function can be established in molecular terms. Four types of information define the quaternary structure of an oligomeric protein. These are (i) the self-association state, (ii) the geometric arrangement of protomers in the associated state, (iii) the symmetry assignment, and (iv) the disposition on the protomer of unique cofactor- or substrate-binding sites relative to the coordinate reference frame of the protein oligomer.

In the preceding paper in this issue (Geiselmann et al., 1992), we studied the association states of the *Escherichia coli* transcription termination factor rho as a function of protein concentration, ionic environment, and binding of oligonucleotide cofactors. By a combination of physicochemical techniques, we showed that in solution the rho protomer is involved in various self-association equilibria [see also Seifried et al. (1991)]. The states of this self-associating system were summarized in the form of a phase diagram with axes defined in terms of protein and salt concentration. Depending on experimental conditions, the average association state of rho was found to range from monomers up to indefinite aggregates.

We also showed (Geiselmann et al., 1992) that under approximately physiological conditions (10-40 μM rho protomers and 50-200 mM KCl) the rho protein exists in a homogeneous

† Portions of this work have been submitted (by J.G.) to the Graduate School of the University of Oregon in partial fulfillment of the requirements for the Ph.D. degree in Chemistry. These studies were supported in part by USPHS Research Grants GM-15792 and GM-29158 (to P.H.v.H.), by NIH Individual Postdoctoral Fellowship GM-10227 (to TDY), and by a grant from the Lucille P. Markey Charitable Trust. P.H.v.H. is an American Cancer Society Research Professor of Chemistry.
* To whom correspondence should be addressed.
‡ Present address: Unité de Physicochimie des Macromolécules Biologiques, Institut Pasteur, 25 rue du Dr. Roux, 75724 Paris Cedex 15, France.
§ Present address: NSF Center for Molecular Biotechnology, Division of Biology (139-74), California Institute of Technology, Pasadena, CA 91125.
‖ Present address: Department of Chemistry, University of California at Riverside, Riverside, CA.

0006-2960/92/0431-121$03.00/0

Table I: Possible Geometries and Symmetry Assignments for the Rho Hexamer [after Klotz et al. (1975)]

geometry	point symmetry	reason for rejection
hexagon	C_6	chemical cross-linking (Figures 2, 3); semidenaturing gel (Figure 4)
hexagon	C_3	association behavior; fluorescence energy transfer
hexagon	C_2	semidenaturing gel (Figure 4); linear Stern–Volmer plot; single fluorescence lifetime; fluorescence energy transfer
hexagon	D_3	not rejected; this is the favored model
trigonal prism	D_3	SAXS, SANS (Geiselmann et al., 1992); EM (Oda & Takanami, 1972); cryo-EM (Gogol et al., 1991)
octagonal	D_3	SAXS, SANS, (Geiselmann et al., 1992); EM (Oda & Takanami, 1972); cryo-EM (Gogol et al., 1991)

hexameric association state. This hexamer most likely represents the major association state in vivo [see Geiselmann et al. (1992) and Seifried et al. (1991)]. Finger and Richardson (1982) had earlier suggested the existence of a hexameric association state for rho on the basis of chemical cross-linking and sucrose gradient sedimentation experiments. The hexameric state appears to be stabilized by RNA. The RNA acts as a cofactor to stimulate an ATPase activity inherent in the rho protein (Finger & Richardson, 1982).

The above results suggest that it is logical to assume a hexameric association state when beginning an investigation of the quaternary structure of rho. Table I lists all possible combinations of geometry and symmetry assignments that can characterize a discrete hexamer species (Klotz et al., 1975). On the basis of small-angle X-ray and neutron scattering (Geiselmann et al., 1992) and electron microscopy (Oda & Takanami, 1972; Gogol et al., 1991), we may unambiguously rule out the (D_3) octahedron and the trigonal prism geometries for the rho hexamer (Klotz et al., 1975). These two geometries are incompatible with our small-angle X-ray scattering (SAXS), small-angle neutron-scattering (SANS), and electron microscopic (EM) data because they have too small a radius of gyration and also because they lack a central hole. Therefore, we are driven to assume a planar hexagonal geometry for the rho hexamer [see also Geiselmann et al. (1992) and Gogol et al. (1991)].

A Basis for Distinguishing between Alternative Symmetry Assignments. A planar hexagonal geometry is compatible with the C_2, C_3, C_6, and D_3 point symmetry groups. C_6 symmetry may readily be distinguished from the alternatives because this symmetry is characterized by only one type of (heterologous) bonding interface between protomers and because the "asymmetric unit" is a single protomer. In contrast, a hexamer with C_3 symmetry has two different bonding interfaces and the "asymmetric unit" is a dimer, while a hexamer with D_3 symmetry has two different, truly isologous,[1] bonding interfaces and the asymmetric unit is a dimer. Finally, a hexamer with C_2 symmetry has three different bonding interfaces, and the asymmetric unit is a trimer.

In the first part of this paper, we present cross-linking and denaturation experiments that examine the interactions between promoters in the rho hexamer. These results are followed by a description of fluorescence-quenching and fluorescence lifetime measurements that we have used to probe the surface accessibility of a dye molecule which is covalently bound at a unique site in each promoter of the hexamer. Finally, we describe fluorescence energy transfer measurements that set a lower limit on the distances that separate the bound dye molecules within the hexamer. The simplest and most coherent interpretation of all our data is that the rho hexamer has D_3 symmetry. The data can conclusively rule out C_6 and C_2 symmetry and can also tentatively rule out C_3 symmetry.

In the second part of this paper, we describe the use of fluorescence energy transfer techniques, together with data from the literature on the tripartite domain structure of the rho promoter and on the "footprint" made by the rho hexamer upon binding to a long molecule of RNA, to determine how the RNA- and ATP-binding sites of rho must be oriented relative to the coordinate reference frame of the hexamer. Using these approaches, we can place significant constraints on the possible relative orientations of these crucial sites.

Materials and Methods

Buffers and Chemicals. We have specified most of the buffers used in these experiments in Geiselmann et al. (1992). The cationic detergents cetyltrimethylammonium bromide (CTAB) and myristyltrimethylammonium bromide (MTAB) were purchased from Sigma. The cross-linking reagent dimethylsuberimidate (DMS) was purchased from Pierce and was stored dry at −20 °C. The high purity acrylamide used as nonionic quenching agent in our fluorescence studies was obtained from American Research Products Co. Spectroscopic grade glycerol was purchased from Aldrich and high purity guanidine hydrochloride from American Research Products Co.

Rho and Oligonucleotide Cofactors. Rho protein and RNA oligonucleotides were purified, stored, and characterized as described in Geiselmann et al. (1992). Rho was fluorescently modified by the method of Seifried et al. (1988). The single cysteine at position 202 in the rho protomer was labeled with either fluorescein or 1,5-IAEDANS to produce species we designate as RHO^{FL-202} or RHO^{AE-202}, respectively. Efficiency of labeling, quantum yield, spectral overlap, and absolute steady-state energy transfer efficiency were all determined by separating the fluorophores of the labeled rho by proteolysis in situ (Epe et al., 1982). Digestion was carried out using 1 μg of Pronase E (Boehringer Mannheim) per milligram of rho protein. The extent of labeling of each rho protomer was determined to be 90–115% (Seifried et al., 1988).

Chemical Cross-Linking. Most chemical cross-linking experiments were performed using the bifunctional cross-linking reagent DMS. A reagent stock solution was prepared by adding 30–46 mg of DMS to 0.9–1.0 mL of an ice-cold solution of 20 or 50 mM HEPES (pH 7.9) and then titrating this solution to pH 8.2 with 4 M KOH. Rho was cross-linked by adding 10–15 μL of this reagent to 35–100 μL of a rho stock solution and incubating at room temperature for 1–10 min (unless otherwise specified). In most cross-linking experiments, the final concentration of rho was 4.3 μM, the final DMS concentration was ~6 mg/mL, and the salt concentration was 0.2 M KCl. In one experiment, SDS was present in the cross-linking reaction at a concentration of 1%. Cross-linking was stopped by adding 5 μL of 1.8 M ethanolamine to the reaction. Finally, 10 μL of 2× electrophoresis loading buffer were added to 10 μL of sample. The resulting solution was immersed in a boiling water bath for 10 min and examined on a polyacrylamide gel.

A 3.6% polyacrylamide slab gel (30:1 acrylamide:bisacrylamide) in 37.5 mM Tris (pH 8.8), 0.1% SDS was used for these studies, with a 2% stacking gel (30:1 acrylamide:

[1] According to the original definition proposed by Monod et al. (1965), a bonding interface corresponds to a pair of complementary surfaces between two protomers. If the bonding interface has a C_2 symmetry axis it is isologous. If it does not have a C_2 symmetry axis it is heterologous.

bisacrylamide) containing 250 mM Tris (pH 6.8, 0.1% SDS. In this gel system, the rho protomer and the bromophenol blue dye front migrate together below the sieving limit of the gel. All gels were stained with Coomassie blue and/or silver as described by Hammes and Rickwood (1981) and were photographed with Polaroid type 55 film. The resulting film negatives were measured with a laser densitometer from Biomed Instruments, Inc.

Semidenaturing Gels. We used electrophoresis in semidenaturing gels (Akin et al., 1985) to analyze the effects of MTAB (and CTAB) on the bonding domains between protomers within the rho hexamer. In this technique the application of a mild denaturant destroys the protomer–protomer contacts at weak bonding interfaces while leaving intact contacts at strong interfaces. In these experiments, we used a 4% polyacrylamide gel (30:1 acrylamide:bisacrylamide) and a running buffer containing 50 mM sodium phosphate (pH 7.8) and 0.1% MTAB (or CTAB).

Fluorescence-Quenching Experiments. Steady-state fluorescence experiments were conducted in the thermostated cell of an SLM-8000 spectrofluorimeter using computerized titration and data capture routines. Glan–Thompson polarizers were used in polarization measurements, after residual excitation polarization arising from the monochrometers was randomized by passage of the light through a quarter-wave plate. All experiments were performed in the photon-counting mode with the observed emission intensity expressed as a ratio to the lamp output intensity. Emission spectra were corrected for photomultiplier response. Other parameters have been described below or elsewhere (Seifried et al., 1988). All experiments contained 1 μM labeled rho unless otherwise noted.

Stern–Volmer quenching curves provide a method for examining the surface accessibility of a dye (Lakowicz, 1983). The steady-state fluorescence intensity was monitored as quenching agent was titrated into the solution. The nonionic quenching agent used in these experiments was acrylamide. The data obtained were analyzed for collisional quenching and for quenching due to complex formation as described by Pesce et al. (1971).

Fluorescence Lifetime Experiments. A very rapidly decaying component of the fluorescence lifetime reflects the Brownian motion of the covalently bound dye molecule within its local environment. This motion was detected and quantitated at 20 °C by time-correlated single photon counting anisotropy measurements. A 750 mW mode-locked 81 kHz continuous wave Nd:YAG laser was used to excite a 6 G cavity dumper (containing 60 mM rhodamine) at 800 kHz. The laser output frequency was doubled and passed through a 310-nm excitation filter. The limiting response time was determined to be 80 ps at half-peak maximum. More than 12000 emission counts were collected over a 4-min period after passage through a 400–500-nm band-pass filter. Data were collected using a Tracor-Northern multichannel analyzer with an 80-ns sweep time, as described by Ruggiero et al. (1989).

Fluorescence Energy Transfer Experiments. The fluorescence energy transfer technique enables one to measure distances beween donor and acceptor fluorophores [see Fairclough and Cantor (1972)]. The observable quantity can be a decrease in fluorescence emission of the donor, an increase in the fluorescence emission of the acceptor, or a decrease in the polarization of the fluorescence emitted by either dye. The maximum distance over which the energy can be transferred, and the efficiency of energy transfer at any given distance, both depend on the spectral overlap between the emission spectrum of the donor and the absorbance spectrum of the acceptor. The overlap integral (J) is defined as

$$J = \int \epsilon_A(\lambda) f_D(\lambda) \lambda^4 \, d\lambda \quad (1)$$

where $\epsilon_A(\lambda)$ and $f_D(\lambda)$ are the wavelength-dependent molar absorptivity and fluorescent quantum yield of the acceptor and donor molecules, respectively. The efficiency of the energy transfer (E) is defined as

$$E = R_0^6/(R_0^6 + R^6) \quad (2)$$

where R_0 is the critical distance over which energy transfer is 50% efficient and R is the measured distance in angstroms.

Since the process described by eqs 1 and 2 is a dipolar energy transfer mechanism, the efficiency of transfer has a sixth-power dependence on the distance between the interacting fluorophores. R_0 can be experimentally determined for any energy transfer system using

$$R_0 = 8.79 \times 10^{-5}(J\kappa^2\eta^{-4}\phi_D)^{1/6} \text{ Å} \quad (3)$$

Equation 3 contains terms for the refractive index of the medium between the interacting chromophores (η), the quantum yield of the donor in the absence of acceptor (ϕ_D), and the orientation parameter (κ^2).

Results

The rho hexamer has the geometry of a regular hexagon [Geiselmann et al. (1992); see also Bear et al. (1988) and Gogol et al. (1991)]. In this paper, we attempt to determine the symmetry of the hexamer. A hexamer with hexagonal geometry could exhibit the four possible point symmetries: C_2, C_3, C_6, or D_3, as indicated in Table I. Certain critical features of these symmetry assignments are shown in the schematic diagrams of Figure 1. In these diagrams, we represent the protomers simply as spheres, because greater resolution is not available from our hydrodynamic, EM, SAXS, and SANS experiments. After establishing the symmetry of the rho hexamer, we attempt to add more detail to the representation of the protomers within the hexamer by drawing on other experimental data.

Symmetry Assignment of the Rho Hexamer Is Consistent with only Certain Hexamer Dissociation Equilibria

C_6 symmetry is unique in that it displays a strict "head-to-tail" arrangement of protomers. All bonding interfaces are of the heterologous A:B type, and the asymmetric unit is the protomer (Klotz et al., 1975). Because there is only one type of bonding interface, the only association states that should be significantly populated are the monomer and the hexamer. Under no conditions should there be dominant populations of dimers, trimers, tetramers, or pentamers (Matthews & Bernhard, 1973; Klotz et al., 1975; Van Holde, 1975).

In contrast, the C_3 and D_3 symmetry groups are each characterized by two different bonding interfaces. In each case the asymmetric unit is a dimer. Under conditions favoring dissociation of the hexamer, we therefore expect to find dominant populations of dimers and tetramers and depleted populations of trimers and pentamers. The interfaces are isologous for D_3 symmetry, and we designate them A:A and B:B. For C_3 symmetry the bonding interfaces are heterologous; the interactions of such bonding interfaces could lead to "indefinite" or unbounded association equilibria for protomers of this symmetry type.

A more complex set of properties is predicted for the C_2 symmetry group. This group is characterized by three different types of bonding interfaces. The asymmetric unit is a trimer.

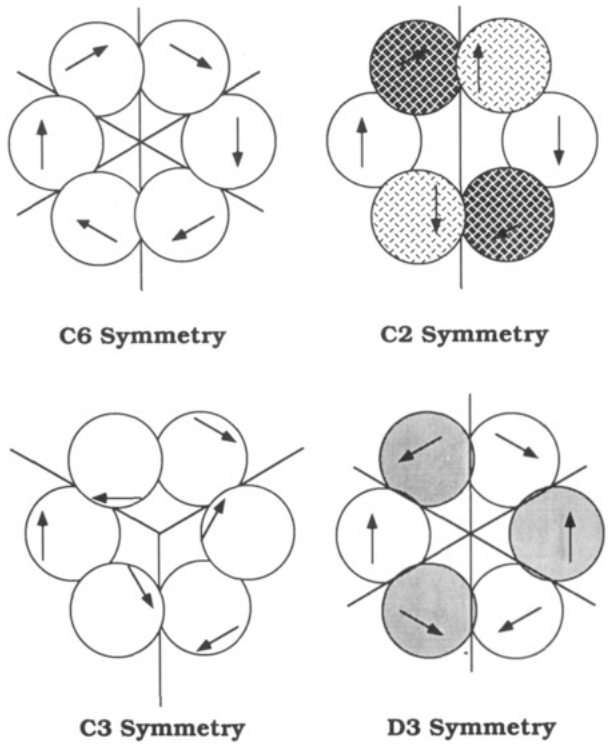

FIGURE 1: Schematic diagrams of four possible symmetry assignments for a planar hexamer of identical protomers. The protomers are represented as spheres that overlap slightly. The shading of each protomer indicates the surface which is visible to the viewer looking down onto the plane of the hexamer, perpendicular to the major 3-fold or 6-fold axis. A different shading indicates a different surface visible to the viewer. An arrow represents a selected stretch of the polypeptide chain of each protomer and indicates the directionality of the polypeptide chain. The lines converging at the center of each hexameric structure indicate a possible separation of the hexamer into asymmetric units. (upper left) The C_6 symmetry group is characterized by one type of bonding interface (heterologous A:B). The asymmetric unit is the monomer. There is one 6-fold rotational axis perpendicular to the plane of the paper. All protomers are face up. (Upper right) The C_2 symmetry group is characterized by three different types of bonding interfaces. The asymmetric unit is the trimer. There is one 2-fold rotational axis through the center of the hexamer, perpendicular to the plane of the paper. Three different faces, or three-dimensional orientations of the protomers, are presented to the viewer. (Lower left) The C_3 symmetry group is characterized by two different types of bonding interfaces. The asymmetric unit is the dimer. There is one 3-fold rotational axis perpendicular to the plane of the paper. All protomers are face up. (Lower right) The D_3 symmetry group is characterized by two different bonding interfaces (isologous A:A and isologous B:B). There is one 3-fold rotational axis perpendicular to the plane of the paper and three 2-fold rotational axes in the plane of the paper. The protomers alternate face up and face down, with three of each orientation. There are true C_2 symmetry axes through all the bonding interfaces in the D_3 structure.

Under conditions favoring dissociation of the hexamers, one might expect to find a significant population of dimers if one type of bonding interface remains strong. If two types of interfaces remain strong, a significant population of trimers should result.

The above arguments predict measurable differences in dissociation behavior for hexamers of the different symmetry groups. Thus techniques that measure the prevalence or stabilities of different association states can be exploited to help establish the symmetry assignment of the rho hexamer.

Chemical Cross-Linking Studies

The symmetry of an oligomeric protein can be studied by covalent cross-linking with a bifunctional reagent, followed by analysis of the cross-linked products on denaturing gels. In principle, the cross-linked products can be resolved as discrete bands and quantitated by densitometry. This method of quaternary structure analysis was pioneered by Davies and Stark (1970) and was first applied to rho by Finger and Richardson (1982).

Highly Cross-Linked Rho Hexamers. As a control for cross-linking efficiency, we conducted experiments under conditions favoring the existence of the stable rho hexamer. These conditions are described in the preceding paper in this issue (Geiselmann et al., 1992). In these experiments, we used the buffer conditions, temperature, and gel system specified by Finger and Richardson (1982). We find, as they did, that extensive cross-linking of the rho hexamer with DMS generates a ladder of bands corresponding to cross-linked dimers, trimers, tetramers, pentamers, and hexamers of the rho protomer. We also have obtained essentially the same results, using a phosphate-based gel system, with the "shorter" bifunctional cross-linking reagents dimethyl adipimidate (DMA) and disuccinimidyl tartarate (DST) (data not shown). We observed cross-linked products larger than the hexamer when high concentrations of rho were reacted with DMS (Figure 3, lane 3). This was expected since rho will form nonspecific aggregates at these high protein concentrations (Geiselmann et al., 1992). These cross-linking reagents all react with primary amines and are expected to cross-link lysine residues at the bonding interfaces between adjacent protomers. The equivalence of the results obtained with cross-linking agents of different length suggests that the reactive lysine residues that lie between rho protomers are in reasonably close proximity. The fact that we observe a ladder of cross-linked products up to the hexamer proves that a cross-link can be formed across each of the six bonding interfaces within the rho hexamer with roughly equal efficiency.

Low Levels of Cross-Linking Produce Two Different Types of Cross-Linked Dimer. The cross-linking technique can be used to generate data of higher resolution involving cross-linked dimers of rho. This can be achieved by decreasing the time of the cross-linking reaction and by analyzing the products on a gel system that gives high resolution in the molecular weight range corresponding to the rho dimer. A typical gel is shown in Figure 2A, and a densitometer scan of the dimer region is presented in Figure 2B. When the cross-linking reaction is quenched after only small number of cross-links have been formed, we observe a doublet of bands of about equal Coomassie staining intensity in the dimer region of the gel. This doublet becomes blurred and merges into one band as cross-linking proceeds further (data not shown).

Limited cross-linking of rho produces a doublet of cross-linked dimers of equal intensities under a variety of experimental conditions. The following parameters were varied: (i) the concentration of rho; (ii) the concentration of KCl; (iii) the concentration of Mg^{2+} or EDTA; (iv) the concentration of cross-linking reagent; and (v) the addition of ATP and/or RNA. Two bands of approximately equal intensity, corresponding to the doublet of dimers, were seen under all conditions wherein the extent of cross-linking was kept low.

The simplest interpretation of these results is that the two dimer bands represent two distinct singly cross-linked species. We suggest that these species differ in electrophoretic mobility because different bonding interfaces are cross-linked. This, in turn, leads to different frictional properties under the "denaturing" conditions that prevail in the gel. Dimers that have been singly and doubly cross-linked across the same interface may be ruled out because we see no difference in the relative intensities of the two dimer bands as a function of the extent of cross-linking (data not shown).

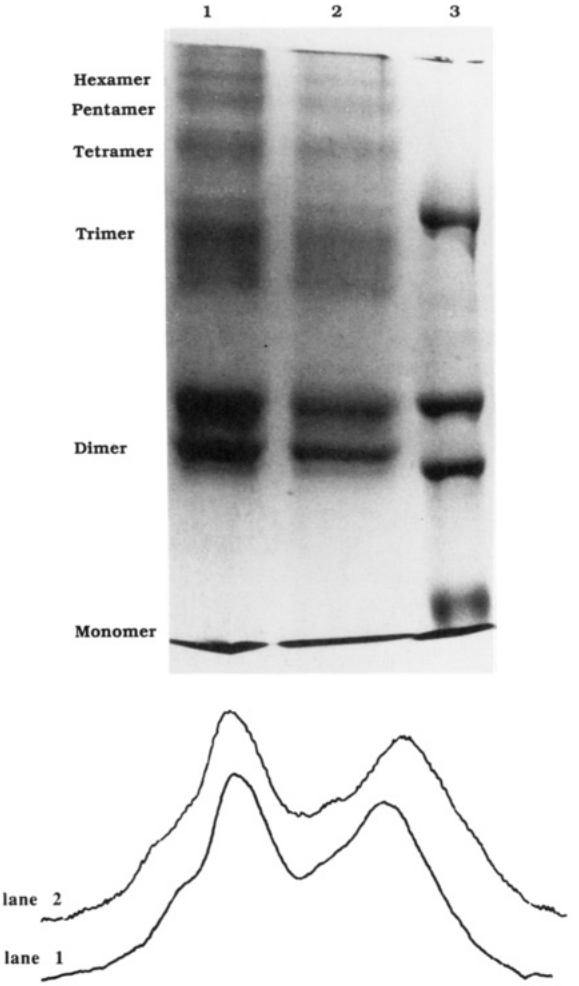

FIGURE 2: SDS–polyacrylamide gel electrophoresis of 4.3 μM rho lightly cross-linked with DMS. (A, top) Coomassie stained gel. Lanes 1 and 2 contain rho protein cross-linked in the presence of 32 or 64 μM ATP, respectively. In addition, 0.2 M KCl and 1 mM EDTA were present in each cross-linking reaction. The cross-linking reactions were continued for 8 min at pH 8.2. Lane 3 contains molecular weight markers at 46 000, 66 200, 92 500, and 116 300. The regions of the gel corresponding to the positions of the monomer, dimer, trimer, tetramer, pentamer, and hexamer bands are marked accordingly. In this gel the molecular weight of the monomer falls below the sieving limit; thus the monomer runs with the dye front. (B, bottom) Densitrometric scan of the dimer region of lanes 1 and 2 from the above gel. The scans show doublets of equal intensity in the dimer region.

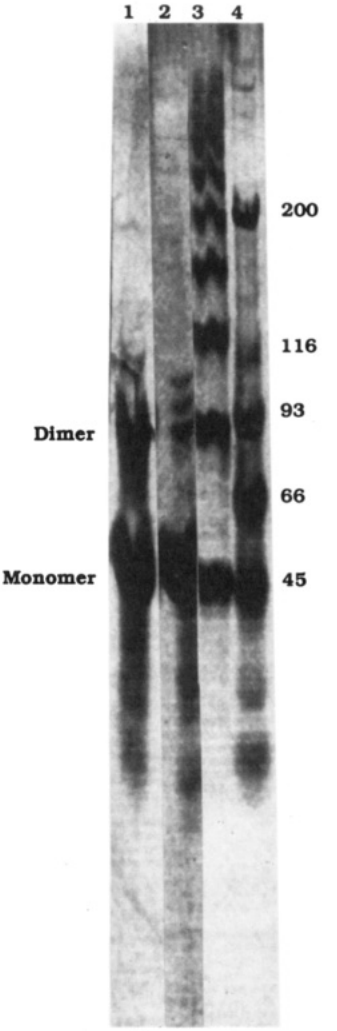

FIGURE 3: Cross-linking of rho with DMS at a protein concentration of 2.2 mg/mL (47 μM rho protomers) in the absence and presence of SDS, and run on an SDS–PAGE gel; see Materials and Methods. (Lane 1) Uncross-linked rho. (Lane 2) Rho cross-linked in the presence of SDS (two bands). (Lane 3) Rho cross-linked in the absence of SDS (six bands plus aggregates). (Lane 4) Molecular weight markers.

This result supports the assignment of C_3 or D_3 symmetry to the rho hexamer, because these symmetries involve two different types of bonding interfaces between protomers. The result also argues strongly against C_6 symmetry, which involves only one type of protomer–protomer contact, and against C_2 symmetry, which involves three different types of bonding interfaces.

Cross-Linking in the Presence of SDS. As indicated above, if the rho hexamer has C_6 symmetry, it must have only one type of bonding interface between protomers. On the other hand, if the hexamer does *not* have C_6 symmetry, then it must display *more* than one type of bonding interface between protomers. For a hexamer with C_3 or D_3 symmetry, disruption of one type of contact should block association past the dimeric state. For a hexamer with C_2 symmetry, disruption of one type of contact should block association past the trimeric state, and disruption of two types of contact should block association past the dimeric state.

In principle, different types of bonding interfaces could exhibit different sensitivities to a denaturant such as SDS. To examine this possibility, we have cross-linked rho in the presence of SDS and have found that only dimeric products are generated at moderately high SDS concentrations. A typical experiment that provides evidence against C_6 symmetry for the rho hexamer is shown in Figure 3. However, this experiment cannot distinguish between the disruption of one type of interface in a structure with C_3 or D_3 symmetry and the disruption of two types of interfaces in a structure characterized by C_2 symmetry.

Electrophoresis on Semidenaturing Gels

One may also use "semidenaturing" conditions with gel electrophoresis to probe the differential stabilities of bonding interfaces (Hammes & Richwood, 1981; Akin et al., 1985). In such experiments, a mild denaturant is present throughout the gel matrix. The native protein oligomer is loaded onto the gel, and as it moves into the denaturant less stable interfaces are disrupted and the protein oligomer partially dissociates.

A suitable denaturant for such studies is the detergent myristyltrimethylammonium bromide (MTAB), which is similar to SDS, but is positively charged and less hydrophobic. Most proteins migrate in an MTAB gel with a mobility proportional to the logarithm of their molecular weight. This result has also been reported for CTAB gels (Akin et al.,

Table II: Steady-state Fluorescence Experiments[a]

fluorescent species	quantum yield	anisotropy (r)	limiting anisotropy	bimolecular quenching constant ($\times 10^{-9}$ M^{-1} s^{-1})
fluorescein	0.93[b]	0.001	0.30[c]	
RHO^{FL-202}	0.28 ± 0.02	0.181 ± 0.05	0.307 ± 0.008	0.82 ± 0.08
+ 0.5 M KCl	0.27	0.175		0.70 ± 0.08
+ poly(rC)	0.25	0.140	0.279 ± 0.007	0.63 ± 0.08
+ 5× rho	0.27	0.175		
digested rho	0.56	−0.008		0.75 ± 0.15[d]

[a] All experiments were performed in 0.1 M KCl, 10 mM $MgCl_2$, and 20 mM HEPES (pH 7.8). [b] Förster (1948). [c] Weber (1954). [d] The labeled protein was denatured in guanidine hydrochloride and the quenching constant was corrected for the increased viscosity due to the denaturant (Lakowicz, 1983).

1985). Although the exact basis of this phenomenon is not clear, it would seem to suggest that (i) enough MTAB is bound to each protein to produce a constant charge/mass ratio, and (ii) the MTAB-complexed proteins all have approximately the same hydrodynamic shape (Reynolds & Tanford, 1970). The molecular weight standards used in the gel shown in Figure 4 migrate exactly as predicted by the logarithmic relationship (correlation coefficient 0.998 for the semilog plot). This calibration curve thus serves to identify the different cross-linked species of rho protomers (see below).

Figure 4 shows a sample of rho that has been loaded (in native form) onto an MTAB gel and then subjected to electrophoresis. It is clear that the rho sample has not been completely dissociated into monomers in this gel. Six bands can be seen in the lane containing the highest concentrations of rho; some bands are fainter than others. We compared to the calibration curve derived from molecular weight standards (see above), these bands run precisely at the positions expected for monomers to hexamers of rho. Since rho is known to form stable hexamers, we have assigned these bands to represent the intermediate association states of rho from monomer to hexamer. The observed distribution of bands becomes biased toward the higher association states at higher concentration loadings of the rho protein, as would be expected for a reversibly associating system. Because we see no smearing of bands, it appears that dissociation equilibria become "frozen" as the rho protein enters the gel.

It is critical to note that the relative intensities of the bands do not follow a geometric series, as would be expected if the rho hexamer had C_6 symmetry. In particular, we see that there is more tetramer than trimer in lane 2 of the gel in Figure 4. The predominance of the tetramer band, together with the relative paucity of the trimer band, argues strongly for the existence of two different types of bonding interfaces between protomers in the rho hexamer. A C_6 symmetry for rho is definitely ruled out by these results. C_2 symmetry can also be ruled out, because a C_2 structure cannot generate more tetramer than trimer (see Figure 1). The only interpretation that is consistent with these data is that the rho hexamer has either C_3 or D_3 symmetry.

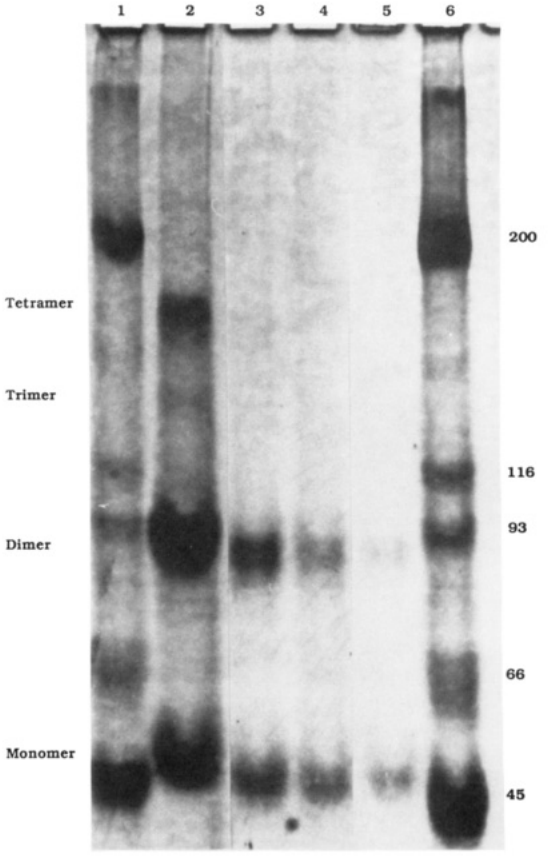

FIGURE 4: Rho protein separated on a semidenaturing (0.1% MTAB) gel as described under Materials and Methods. Lanes 1 and 6 contain molecular weight markers. Lanes 2 through 5 contain 10-μL loads of decreasing concentration of rho protein (21.5, 10.75, 5, 2.5, and 1.25 μM, respectively). In lane 2, the monomer, dimer, and tetramer states are clearly more populated than the trimer, pentamer, and hexamer states.

Fluorescence-Quenching and Fluorescence Lifetime Experiments

Fluorescence experiments were performed to gather additional symmetry information and to limit the possible orientations of various unique sites (ATP- and RNA-binding) sites) within the rho hexamer.

Fluorescence-quenching experiments can provide a sensitive test for nonequivalent fluorophore environments. In our experiments a single fluorescein molecule was covalently attached to the single (nonessential) cysteine residue of the rho protomer. (Stoichiometry of labeling determinations yielded values of 0.9–1.15 dyes per rho monomer; see Materials and Methods.) Thus a maximum of one dye adduct is bound per rho protomer, and a test for nonequivalent fluorophore environments can provide information about the symmetry of the distribution of protomers within the hexamer.

Experiments were conducted with acrylamide as a quenching agent. A control experiment showed that rho retains ATPase activity in the presence of the maximum concentration of acrylamide used in these experiments. Titration of rho with acrylamide was monitored by measurement of fluorescence intensity. Titration curves were obtained in 0.1 M KCl and in 0.5 M KCl, in either the presence or the absence poly(rC). The labeled protein was denatured in 8 M guanidine hydrochloride, and a quenching curve was determined. The bimolecular quenching constant was corrected for viscosity differences between guanidine and buffer solutions. In all cases a strict linearity of Stern–Volmer plots was observed, which indicates that the system can be described with a single collisional quenching constant and that complexes are not formed

Table III: Time-Resolved Fluorescence Experiments[a]

fluorescent species	lifetime (ns)	amplitude (%)	rotational correlation time (ns)
RHO^{Fl-202}	3.86 ± 0.01	97	
	1.80 ± 0.28	3	
BSA^{Fl} [b]	3.86		
BSA^{AE} [b]	23.5	82.3	
	11.25	17.7	
RHO^{AE-202}	17.5 ± 0.08	79	154 ± 11
	6.7 ± 0.11	20	
	0.72 ± 0.03	1	
+0.5 M KCl	17.5 ± 0.06	77	124 ± 8
	6.9 ± 0.11	22	
	0.67 ± 0.03	1	
+poly(rC)	17.2 ± 0.06	77	290 ± 35
	7.3 ± 0.13	21	
	0.77 ± 0.02	2	

[a] All experiments were performed in 0.1 M KCl, 10 mM $MgCL_2$, and 20 mM HEPES (pH 7.8). [b] BSA was labeled with the fluorescein or 1,5-IAEDANS, and the lifetimes were recorded (Chen & Scott, 1985).

between the protein and the acrylamide. The observed bimolecular quenching constants (Table II) are the same, within error, for all solution conditions except for the sample containing poly(rC).

This finding leads to four conclusions. (i) The dye adduct cannot be buried deeply in the interior of the rho protomer, since this would render it inaccessible to the quenching agent. Also, the solvent accessibility of the dye in the native protein is quite similar to that of the dye adduct on the denatured polypeptide. Thus the dye adduct must lie at the surface of the rho protomer, even when protomers are associated in the hexamer structure. (ii) The dye experiences only a single surface accessibility environment in the rho hexamer and any dissociation intermediates that may be induced at high KCl concentrations. This argues against C_2 symmetry, for which at least two fluorophore environments are expected.[2] Therefore, the fluorescence quenching data are consistent with C_6 and D_3 symmetries, for which only a single fluorophore environment is expected in the hexamer (see Figure 1). (iii) The rho hexamer can be partially dissociated by increasing the salt concentration of the solution (Geiselmann et al., 1992; Seifried et al., 1991). The surface accessibility of the fluorophore does not change as salt concentrations are increased to bring about partial dissociation, which indicates that the fluorescent dye cannot lie at the A:B interface in a C_6 structure or at the weaker of the two interfaces (A:A or B:B) in a C_3 or a D_3 structure. (iv) The dye is apparently flexibly attached to the protein, since we obtain a quenching constant close to that seen with the dye adduct on the denatured protein chains. This observation has implications in the fluorescence energy transfer experiments discussed below.

The validity, sensitivity, and the interpretations of this technique that we put forward here are supported by results obtained with rho samples complexed with poly(rC). The reduced collisional rate observed with such complexes (see Table III) compared to the uncomplexed rho samples described above probably reflects a combination of a decreased rotational freedom of the dye adduct within the protein–polynucleotide complexes and increased screening of the adduct (from quencher) as a consequence of interhexamer aggregation in such systems [see Bear et al. (1988), Gogol et al. (1991), and below].

Symmetry information may also be deduced from measurements of fluorescence lifetimes. This approach is related and complementary to the fluorescence-quenching technique described above. If only a single fluorescence lifetime is measured, then there must be only one type of environment available to accept energy from the excited fluorophore. We observe only a single fluorescent lifetime for fluorescein-labeled rho in isotropic decay measurements (Table III). This single lifetime is observed in both 0.1 M KCl and 0.5 M KCl, and in the absence or presence of poly(rC).

To further test for different fluorophore environments, samples of rho were also labeled with 1,5-IAEDANS, which has a biexponential fluorescence intensity decay curve. These two lifetimes are an intrinsic property of the dye. The relative intensities and lifetimes of this dye attached to rho remained invariant as the buffer environments and association states of rho were changed (Table III). We conclude from all these fluorescent lifetime and fluorescence-quenching experiments that there is only one environment for the relatively mobile dye under all these conditions. Of course, it remains possible in principle that the dye adducts could reside in two (or more) different environments, but it is improbable that such environments would be equivalent both in solvent accessibility and in electronic interactions.

Fluorescence Energy Transfer Experiments

We have performed an additional type of experiment that argues against a C_2 symmetry assignment for the rho hexamer and further limits the location of the dye molecule. Identical molecules of a dye (e.g., fluorescein) can undergo a nonradiative energy transfer of the Förster type, as described previously (Seifried et al., 1988). The energy transfer efficiency (E) is a function of the critical separation distance (R_0) and the actual separation distance (R) between the dye molecules, as described in eqs 2 and 3.

A complicating factor in energy transfer measurements is the orientation parameter κ^2. This parameter is related to the relative geometries of the emission dipole of the donor and the excitation dipole of the acceptor. The κ^2 parameter cannot be easily measured; however, many discussions of fluorescence energy transfer have concluded that this factor is unlikely to be significant in systems such as ours because of the improbability that the dyes are both immobile and restricted in the most unfavorable geometry. We have looked for evidence of dye mobility within rho oligomers in order to assess the possibility of simultaneous dye rigidity and unfavorable interchromophore dipole orientation.

We interpret the results from time-correlated anisotropy measurements of RHO^{AE-202} (Table III) as reflecting localized motion of the dye on the surface of the protomer. This motion is fast relative to the diffusional motion expected for the rho oligomer. Thus under low salt conditions (0.1 M KCl), in which rho exists primarily as a hexamer (Geiselmann et al., 1992; Seifried et al., 1991), the observed isotropic rotational correlation times measured for the rho^{AE-202} correspond to those expected for a sphere of the size of a 1.3-mer of rho protomers [see Seifried et al. (1991)]. Increasing the salt concentration decreases somewhat the apparent average molecular weight of the rho samples (Seifried et al., 1991); under these conditions the isotropic rotational correlation times correspond to those expected for an isolated spherical rho protomer. Since the actual rho oligomers within which these fluorescent adducts are located are clearly much larger, these

[2] These fluorescence data are not informative with respect to the possibity of C_3 symmetry. Depending on the location of the bound dye on the protomer, either one or two fluorescent environments would be expected for this symmetry class. See Figure 1 for details.

results suggest that the dye adduct retains significant rotational freedom of motion in its attachment to the protein.

To test the validity of this conclusion, we complexed rho hexamers with long poly(rC) molecules, which has been shown to lead to the formation of large intertwined aggregates as visualized by conventional and cryoelectron microscopy (Bear et al. 1988; Gogol et al., 1991). Here the calculated rotational correlation time of the dye from anisotropic decay measurements yields an apparent spherical molecular weight of a 2.5-mer of rho. Clearly, in these aggregated complexes, the fluorescent adduct has lost some of its rotatory freedom. However, we can also conclude from all these results that the dye adduct is not held rigidly against the protein surface and has a high-frequency motional component. This conclusion is corroborated by the high collisional quenching rates discussed above. For these reasons, we conclude that the orientation factor cannot be responsible for the fact that we see no fluorescence energy transfer in the labeled rho system.

A standard method for detecting and quantitating fluorescence energy transfer is to measure the quantum yield of the donor fluorescence. When energy transfer occurs, this parameter decreases. Under no conditions did we observe a decrease of donor quantum yield in experiments with the labeled rho protein (Table II). Another indication of energy transfer is a decrease in fluorescence lifetime due to the increased relaxation of the dye through nonradiative transfer. As discussed above, a single invariant lifetime was observed for the fluorescein-labeled rho under several different conditions that are expected to affect the association state of the molecule. The critical distance for fluorescein self-energy transfer was determined to be 45 Å. Therefore all the sites within the hexamer that are labeled by fluorescein must be more than 45 Å apart.

Protomer Mixing Experiments. Completely labeled RHO^{FL-202} was mixed with unlabeled rho in an effort to decrease the average number of labeled subunits per hexamer and thus to decrease any capacity for self-energy transfer. Subunits were mixed either in the native or in the denatured state (followed by renaturation). Such mixing experiments assume that a free exchange of subunits occurs in solution. This assumption is supported by the subunit exchange experiments of Ruteshouser and Richardson (1986), by studies of the assembly pathway of the rho hexamer (Seifried et al., 1991), and by experiments involving the mixing of active and photoinactivated rho subunits (Seifried, unpublished results).

Denaturation was carried out at high protein concentration by the addition of 8 M urea and 20 mM β-mercaptoethanol. The rho protein renatured when the urea concentration was rapidly diluted to 7 mM. More than 70% of the intrinsic ATPase activity was recovered, provided that the denatured material was renatured within 30 min. The polarized fluorescence of the renatured RHO^{FL-202} was identical to that of the native material (Table II). No self-energy transfer was observed in these samples, either immediately after renaturation or after an additional 8 h of incubation.

Dye Pair Experiments. Rho was also labeled at Cys-202 with 1,5-IAEDANS, to yield RHO^{AE-202}, as described by Seifried et al. (1988). This material was mixed with RHO^{FL-202}. Fluorescein and IAEDANS form a Förster dye pair with a critical distance of 37 Å. Under no experimental conditions did we observe a quenching of donor fluorescence or an enhancement of acceptor fluorescence using rho labeled with this dye pair. Subunit mixing experiments and denaturation/renaturation experiments were performed at several different molar ratios of labeled to unlabeled rho, as well as over a range of different salt and protein concentrations. No energy transfer was seen in any of these experiments.

Depolarization Measurements. Energy transfer produces a depolarization of fluorescence. This fact can be rationalized as follows. If donor and acceptor fluorophores are identical (fluorescein) and are close enough together to participate in resonance energy transfer, and if one of the dyes becomes excited, then energy can be transferred nonradiatively before being emitted as fluorescence. If the relative orientations of the donor and the acceptor transition dipoles are not rigidly fixed, which we have shown above to be true, then the transferred energy that is finally emitted as fluorescence from the acceptor will no longer be parallel to the emission dipole of the donor. This results in depolarization of fluorescence (Pesce et al., 1971).

We tested for such depolarization in several ways (Table II) but failed to observe any. (i) Steady-state polarization (anisotropy) was monitored in the same experiments that were used to look for donor quenching. (ii) Fluorescently labeled subunits of rho were diluted with unlabeled rho by mixing or denaturation/renaturation techniques. (iii) The association state of the rho was perturbed by the addition of poly(rC) or salt. In no case was there significant change in polarization. Again, the only exception to this result was obtained with rho complexed with poly(rC) (see above). Here the decreased anisotropy observed most likely does reflect fluorescence energy transfer, since an increase in rotational correlation time caused by aggregate formation would be expected to increase the fluorescence polarization, rather than bringing about the decrease observed (Table II).

Perrin plots were constructed to determine apparent limiting anisotropies. In a Perrin plot, one varies the viscosity of the solution and monitors polarization. At infinite viscosity a limiting anisotropy is obtained that is determined by the electronic structure of the fluorophore. If energy transfer occurs, then an additional depolarization component would result in a reduced apparent limiting anisotropy. We found limiting anisotropies to be identical for literature value (Weber, 1954), for free fluorescein, and for labeled rho under a variety of solution conditions. This further supports our conclusion that no fluorescence energy transfer takes place. As expected, a small but significant change in limiting anisotropy was observed with the sample containing poly(rC), further strengthening the argument for a small amount of energy transfer under these conditions and again verifying the validity of our interpretations of this technique.

Changing the Association State of The Rho. Labeling of rho at Cys-202 does not significantly affect the association state of rho, as determined by quasielastic light-scattering experiments and HPLC gel filtration experiments (Seifried et al., 1991). Salt and protein concentration were varied to perturb the association state of rho, and no evidence of energy transfer was observed (Table II). Complexing rho with long poly(rC) chains drives rho largely to the hexameric state but also induces aggregate formation, as indicated above. This manipulation does induce a small amount of energy transfer. The donor quantum yield decreases by 10%, collisional quenching rates are decreased, and some depolarization of fluorescence is observed (Table III). The magnitudes of these changes are small but significant. We believe that the small amount of energy transfer observed in these experiments may well reflect interhexamer energy transfer between hexamers within these aggregates. This also, of course, strengthens our conclusion that the dye adducts attached to rho have some rotational freedom and thus that it is not the orientation factor that

prevents energy transfer between dye adducts within a single hexamer.

Conclusions from Fluorescence Energy Transfer Experiments

The energy transfer experiments allow us to conclude with confidence that no two dye molecules within the rho hexamer lie closer together than the critical distance (R_0 = 45 Å). This represents a very conservative minimum distance estimate. This requirement significantly limits the possible locations of the dye adducts within promoters arranged in a D_3 symmetry and makes it very difficult to justify a C_2 or a C_3 arrangement. Fluorescence quenching and lifetime experiments provide additional evidence against the C_2 form, since only one fluorophore environment is observed and a C_2 arrangement would predict two different environments.

Finally, we use fluorescence data to consider how the various unique sites on the rho protomer (e.g., the ATP- and RNA-binding sites) are oriented relative to the coordinate reference frame of the hexamer. These fluorescent measurements reveal only a single fluorophore environment, even under conditions that allow the rho hexamer to dissociate (see above). This result implies that, in a D_3 structure, the dye molecules cannot be bound at the weaker of the two types of bonding interfaces. If bound in such a location, the quenching of the fluorophore would have to change upon hexamer dissociation, which is not observed.

A more severe constraint on protomer orientation is provided by the fluorescence energy transfer data. Our failure to observe self-energy transfer indicates that, in the rho hexamer, the dye molecules must lie significantly farther apart than the R_0 distance; i.e., 45 Å for these fluorescein dye pairs. The allowed locations for the dye molecules in the D_3 hexamer (that remain available after taking these constraints into account) are indicated by the clear areas representing the ATP domain in the D_3 representation of Figure 5 (see Discussion).

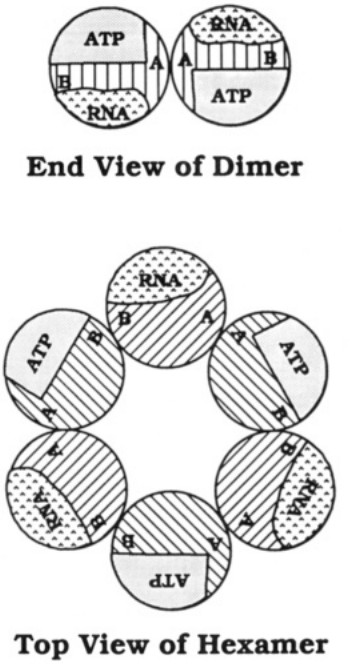

FIGURE 5: Schematic views of the rho hexamer and dimer asymmetric unit. The three domains of the protomer are represented with different shading. The ATP-binding domain can also be considered the fluorescent label domain. The end view of a dimer of protomers is the deduced low-resolution representation of the three-dimensional organization of the polymer-binding domains, ATP-binding domain, and two different protomer-interaction domains. This is a side view, looking along the plane of the hexamer from the outside diameter toward the center of the hexamer. The top view is a representation of the hexamer as might be seen looking down on the hexamer, viewing along the axis perpendicular to the main plane of the hexamer. We use 48 Å for the diameter of the protomers and 90 Å for the distance between the centers of opposite protomers within the hexamer [see text, Geiselmann et al. (1992), Gogol et al. (1991), and Seifried et al. (1991)].

DISCUSSION

Rho protein is an essential transcription termination factor in *E. coli*. It is hypothesized that this protein acts by binding as a hexamer to a nascent RNA transcript. Electron microscopy (Bear et al., 1988; Gogol et al., 1991), neutron scattering (Geiselmann et al., 1992), and RNA titration studies (McSwiggen et al., 1988) support the view that the RNA becomes wrapped around the outside of the rho hexamer during the initial binding event. It is thought that the rho hexamer then moves toward the 3′ end of the RNA and eventually releases the RNA from the transcription complex by means of an RNA–DNA helicase activity (Brennan et al., 1987). The helicase activity of rho, and presumably also its translocation along the RNA, depends on the hydrolysis of nucleotide triphosphates (Brennan et al., 1987).

To develop a molecular model of how the rho hexamer might discharge its function, we need first to determine the quaternary structure of the hexamer. In the preceding paper in this issue (Geiselmann et al., 1992), we have shown that the rho hexamer has a planar hexagonal geometry. Two additional structural features remain to be determined. These are (i) the symmetry properties of the hexamer, and (ii) the orientation of the protomers relative to the coordinate reference frame of the hexamer. Both of these features are determined in this paper.

Symmetry of the Rho Hexamer

As outlined above, a hexamer of planar hexagonal geometry must, in principle, fall into one of the following symmetry classes: C_2, C_3, C_6, or D_3. Symmetry assignments can be made directly by X-ray crystallography. However, to out knowledge, diffraction-quality crystals of rho protein, either alone or as a complex with RNA or DNA oligomers, have not yet been successfully prepared. Thus we are forced to turn to less direct techniques to determine the symmetry of the rho hexamer. In this paper we consider data from chemical cross-linking, electrophoresis in semidenaturing gels, fluorescence quenching, fluorescence lifetime, and fluorescence energy transfer measurements. We strongly favor a D_3 symmetry assignment for the rho hexamer for the following reasons.

Low Extents of Chemical Cross-Linking. At low extents of cross-linking with DMS we observe a doublet of equally intense bands in the region of the gel where a cross-linked dimer of rho protomers should run (Figure 2). The simplest interpretation of this observation is that two different classes of cross-linked dimer are generated by single cross-links across two different bonding interfaces between protomers. This interpretation argues against a C_6 symmetry assignment, since a C_6 hexamer would have only a single type of bonding interface and should therefore produce only a single type of cross-linked dimer. It also argues against C_2 symmetry, which would have three types of bonding interfaces and thus should produce three types of cross-linked dimer.

We can dismiss the argument that the two dimer bands seen in Figure 2 represent species that are singly and doubly cross-linked across the same bonding interface. The two bands are always of equal intensity, which is inconsistent with this interpretation. Similarly, one cannot argue that the doublet

of dimers in Figure 2 results from two *different* cross-links across a single type of bonding interface. If this were the case one would expect to see also a faint third band in the dimer region of the gel, corresponding to a rho dimer that contains both types of cross-link. Such a band was not seen in our DMS cross-linking reactions under any conditions.[3]

Chemical Cross-Linking in SDS. We have obtained additional evidence against a C_6 assignment by conducting chemical cross-linking experiments in the presence of SDS (Figure 3). We find, in such experiments, that no species larger than dimers is generated by cross-linking. This experiment again suggests that more than one type of bonding interface exists between protomers in the rho hexamer and that only one type of bonding interface is stable in the presence of SDS. We note that this experiment can provide no information on the number of different types of interfaces in the intact rho hexamer, except to say that there is more than one type. Thus this experiment cannot discriminate between C_2, C_3, and D_3 symmetries.

Semidenaturing Gels. The detergent MTAB is less potent in disrupting hydrophobic bonds than SDS and, because it is charged, can be used in gel electrophoresis in a manner very analogous to SDS. We have confirmed that the mobility of proteins in semidenaturing MTAB gels is proportional to the logarithm of their molecular weight [see Akin et al. (1985)]. We have loaded the native rho protein into such a gel (Figure 4) and clearly see the presence of rho monomers, dimers, and tetramers. Trimer, pentamer, and hexamer bands are faint or absent depending on the concentration of rho. Six bands can be seen at the highest rho concentration (Figure 4, lane 2). The bands are located where they are predicted to electrophorese, on the basis of the molecular weight of the oligomer species, and can therefore be assigned to the monomer, dimer, trimer, tetramer, pentamer, and hexamer states of rho. The proportion of the different species depends on the concentration of rho loaded on the gel, with the higher association states favored at higher rho concentrations. This behavior is expected for a reversibly self-associating system [see also Seifried et al. (1991)].

The most critical feature of Figure 4 is the paucity of trimers, compared to dimers and tetramers. This observation provides strong evidence against C_6 symmetry, which should result in monotonically decreasing band intensities. This particular feature of Figure 4 also argues against a C_2 symmetry assignment. A C_2 assignment will have a trimer as the asymmetric unit and thus would predict more trimers than tetramers. This follows because only two types of bonding interfaces must be intact to yield a trimer, while three bonding interfaces must be intact to yield a tetramer. The results from the semidenaturing gel experiments are therefore consistent only with a C_3 or D_3 symmetry assignment.

One might expect to obtain an additional free energy gain from closure of the hexamer ring in an oligomer characterized by C_3 or D_3 symmetry. This would result in a predominance of hexamers over tetramers, which is not observed in Figure 4. Cryoelectron microscopy studies (Gogol et al., 1991) reveal a large population of "notched" hexamers, which has been interpreted as hexamers in which ring closure has not taken place. Studies of the association behavior of rho (Seifried et al., 1991) show the dimer to tetramer association constant to be roughly equal to the tetramer to hexamer association constant. This demonstrates that ring closure in the rho system does not lead to a free energy gain. On the contrary, the data suggest that ring closure induces a strain into the hexamer, with the open (notched) hexamer comprising a stable thermodynamic entity. The relative intensities of tetramer and hexamer in Figure 4 support this conclusion.

Fluorescence Quenching and Fluorescence Lifetime Measurements. We have bound fluorescein covalently to a unique site in the rho protomer. Our experiments address whether the bound dye is buried in the interior of the protomer or is located at the surface and also whether only one environment is encountered by the dye adducts. The fact that the fluorescence can be efficiently quenched by acrylamide in solution indicates that the dye must lie at the surface of the protomer in a solvent-accessible location. C_6 and D_3 symmetry assignments predict a single surface environment for the dye, while a C_2 symmetry assignment would predict two or more surface environments. A C_3 symmetry assignment predicts either one or two surface environments, depending on where the dye is bound. Experimentally, we see only one quenching constant in Stern–Volmer plots. We also measure only a single fluorescence lifetime and observe only one rotational correlation time in anisotropy decay measurements. These experiments are therefore consistent with a single fluorophore surface environment and argue against a C_2 symmetry.

A D_3 Assignment is Most Consistent with Other Data. A D_3 symmetry assignment requires that the rho hexamer consist of three identical dimers. This symmetry is also consistent with the following properties of rho, all of which suggest an isologously bonded dimer as the asymmetric unit within the functional hexamer. (i) The stoichiometry of ATP binding has been reported to be three molecules of ATP per rho hexamer (Stitt, 1988). We have extended this work and find two classes of sites on the rho hexamer, consisting of three strong bonding sites and three weak binding sites (Geiselmann and von Hippel, manuscript in preparation). (ii) The ATPase activity of a mixture of wild-type and mutant rho protein depends on interactions between two (or possibly three) protomers within the hexamer and cannot simply be a property of independent protomers (Richardson & Ruteshouser, 1986). (iii) A limiting sedimentation coefficient of 4.3 S is observed in sucrose gradients as the concentration of rho is decreased (Finger & Richardson, 1982; Seifried et al., 1991), indicating the presence of a stably associated species larger than rho monomers. Hydrodynamic calculations, based either on an empirical relationship between sedimentation coefficient and molecular weight (Van Holde, 1975) or on Kirkwood–Reismann theory (Bloomfield et al., 1967), indicate that this sedimentation coefficient is too large to represent the rho monomer and thus probably corresponds to a dimer of rho (calculations not shown). This suggests that the dimer is the predominant species in dilute solutions of rho. This point is explored further elsewhere (Seifried et al., 1991). (iv) The binding of short RNA or DNA oligomers to the rho hexamer displays a strong binding stoichiometry of one oligomer per two rho protomers. This binding interactions induces rho hexamers to dimerize to dodecamers (Geiselmann et al., 1992). (v) The ATPase activity of rho behaves as if the functional ATPase unit is a dimer of rho protomers (Seifried et al., manuscript in preparation). (vi) Rho forms a simple stable hexamer association state under the appropriate solution conditions. This argues against a C_3 symmetry assignment since this symmetry would be expected to lead to complicated ("branched") associated species due to the large number of

[3] Of course the existence of very special geometrical circumstances in any of the symmetry classes considered could lead to the observed doublet of dimers. Therefore this result alone does not conclusively rule out C_6 or C_2 symmetry. Nevertheless, the entirety of our data presented to this point is most easily explained with a D_3 symmetry assignment for the rho hexamer.

different types of contact surfaces that are present. No such species have been observed in our electron microscopy studies (Bear et al., 1988; Gogol et al., 1991).

Summary of Symmetry Considerations. The data presented above conclusively rule out both a C_6 and a C_2 symmetry assignment for the rho hexamer. We cannot definitively rule out C_3 symmetry, but the combination of all available data (including fluorescent energy transfer) makes this symmetry seem unlikely. A hexamer with C_3 symmetry would use four different intersubunit contacts to form the two bonding interfaces. In contrast, a hexamer characterized by D_3 or C_6 symmetry would use only two intersubunit contacts. Four distinct contact surfaces might be hard to accommodate within the relatively small rho protomer, which carries at least two other functional domains (see below). In addition, this large number of potential intersubunit contact points could easily lead to alternate complicated association states. For these reasons Klotz et al. (1975) do not even consider this symmetry as a possibility for a hexamer. None of the available data suggest such complexities. It appears that D_3 is the only symmetry class that is consistent with all the known facts about the rho hexamer (see Table I).

The "up–down–up–down–up–down" pattern characteristic of D_3 symmetry (see Figures 1 and 5) is based on the rho dimer as the asymmetric unit. The dimers are related to each other through a 3-fold rotation axis perpendicular to the plane of the hexamer. Each dimer is composed of identical protomers related to one another through an isologous bonding interface and an exact C_2 axis of symmetry. The D_3 symmetry also involves a second homologous bonding interface (B:B) between adjacent dimers.

Orientation of Protomers Relative to the Coordinate Reference Frame of the Hexamer

The final aspect of quaternary structure that remains to be specified is the disposition of certain unique features on the rho protomer (i.e., the ATP- and RNA-binding sites) relative to the coordinate reference frame of the hexamer. In this section, we show that a strong constraint on this aspect of the quaternary structure can be deduced by combining data from several different experimental approaches.

Fluorescence Energy Transfer Measurements. Fluorescein can engage in self-energy transfer. It has been determined that the critical Förster distance for such transfer with RHO^{FL-202} is 45 Å [see Seifried et al. (1988)]. However, in the experiments described in this paper, no inter-fluorescein self-energy transfer is observed within the rho hexamer. The lack of significant energy transfer has been shown in several ways. (i) No fluorescence depolarization is observed. (ii) There is no change in fluorescence intensity as the proportion of labeled rho protomers within the rho hexamer is decreased by exchange with a pool of unlabeled rho. (iii) No change in fluorescence intensity is observed as the salt concentration is increased to promote hexamer dissociation. (iv) No change in fluorescence intensity is observed in *dilute* solutions of rho when poly(rC) is added to promote hexamer assembly.[4] (v) No energy transfer is observed within rho hexamers carrying two types of labeled rho protomers (RHO^{FL-202} and $RHO^{IAEDANS-202}$ as acceptor and donor). (vi) Perrin plots were constructed to determine if, under conditions favoring rho association, a limiting anisotropy less than that of free fluorescein might be observed due to energy transfer. High and low salt and protein concentrations all yield similar limiting anisotropies, which are identical within error to the values measured with free fluorescein.

ATP-Binding Sites. We have argued above that in the rho hexamer fluorescence energy transfer is not likely to be disallowed by severely unfavorable orientation (κ^2) effects. We would therefore expect to observe some energy transfer if the separation between any two dye molecules within the rho hexamer were equal to, or less than, the critical Förster distance (~45 Å). The rho hexamer has been shown to be ~135 Å in diameter and ~48 Å thick (Geiselmann et al., 1992). We conclude that the fluorescein dye adducts must be restricted to certain locations within the hexamer. Since the site of fluorescent labeling is located quite near the ATP-binding site of rho (Seifried et al., 1988; Dombrowski & Platt, 1988), the dye binding site can be used to represent the ATP-binding site in a low-resolution model of the quaternary structure. This constraint on the quaternary structure of the D_3 hexamer is depicted in Figure 5.

In a D_3 structure, identical points on rho protomers will be separated by greater distances than for any other symmetry class. In this symmetry arrangement, the dye molecules can be placed alternatively at the tops and at the bottoms of adjacent rho protomers, which allows the dye molecules to lie as much as 68 Å from one another. This distance is consistent with our results, since it lies beyond the limit of detection of fluorescein self-energy transfer experiments.

RNA-Binding Sites. On the basis of nuclease-digestion studies (Dombrowski & Platt, 1988), electron microscopy (Gogol et al., 1991), and contrast-variation small-angle neutron scattering (Geiselmann et al., 1992), the RNA is believed to bind at the outer periphery of the rho hexamer. If the hexamer has D_3 symmetry, then all six RNA-binding sites must be located at the outer periphery of the hexamer. This arrangement can be visualized by letting the arrows in the D_3 model of Figure 1 represent the RNA-binding sites.

It is possible to locate the RNA-binding sites of the individual rho protomers alternatively on the top and on the bottom of a rho hexamer with D_3 symmetry. This arrangement is confirmed by the observation (Geiselmann et al., 1992) that, in the presence of short RNA oligonucleotides, rho forms a homogeneous dodecamer with the RNA (three RNA oligomers per rho hexamer) located at the periphery of the molecule (Geiselmann et al., 1992). The RNA-binding sites at the interaction surface *between* the pairs of hexamers comprising the dodecamer are occluded, and RNA can only bind to the outer binding sites. This explains the observed stoichiometry of three short RNA ligands per rho hexamer. The RNA bound at the outside of the dodecamer further limits association via the top or bottom faces of this structure. These association data, as well as coupled conformational changes within a dimer, are most consistent with a D_3 symmetry for the rho hexamer and are described in detail elsewhere (Geiselmann et al., manuscript in preparation).

Tripartite Domain Structure. The rho protomer has three distinct structural domains that can be separated by trypsin cleavage (Engel & Richardson, 1984; Bear et al., 1985; Platt et al., 1989, 1990; Dolan et al., 1990). (i) The RNA-binding domain resides in the N-terminal 151 amino acids of the polypeptide chain (Dombrowski & Platt, 1988). (ii) The ATP-binding domain resides in the central part of the protomer sequence, corresponding to amino acid residues 150–350 (Platt et al., 1989). This domain has sequence homology with known

[4] However (see Results), some interhexamer self-energy transfer *is* observed when high concentration of labeled rho are assembled into contiguous hexamers on long poly(rC) molecules, thus validating our interpretations by showing that self-energy transfer can (as expected) be observed in this system when interdye adduct distances are small enough.

ATP-binding domains (Dombrowski & Platt, 1988). The binding site of the fluorescein dye (Cys-202) lies within this domain. (iii) The carboxyl-terminal domain (amino acid residues 351–419) most likely participates in at least one of the types of bonding interfaces that stabilize the D_3 hexamer (Platt et al., 1989).

An Integrated View. These various data now permit us to propose an integrated model for how the rho protomers are oriented relative to the coordinate reference frame of the hexamer. A schematic diagram of this model is presented in Figure 5, which shows an asymmetric unit dimer of rho protomers oriented within the D_3 hexamer. Each monomer is represented as a three-domain structure as defined above. The bonding interfaces, ATP-binding sites, and RNA-binding sites are indicated. This model is consistent with all available data on the quaternary structure of the rho hexamer. Although this model is relatively crude and will certainly be refined by future experiments, we believe that it represents all the essential aspects of the quaternary structure of the rho hexamer that are needed to formulate a physical mechanism for rho action. Such a mechanism will be presented elsewhere (Geiselmann et al., manuscript in preparation).

Registry No. 5′-ATP, 56-65-5.

References

Akin, D. T., Shapira, R., & Kinkade, J. M., Jr. (1985) *Anal. Biochem. 145*, 170–176.

Bear, D. G., Andres, C. L., Singer, J. D., Morgan, W. D., Grant, R. A., von Hippel, P. H., & Platt, T. (1985) *Proc. Natl. Acad. Sci. U.S.A. 82*, 1911–1915.

Bear, D. G., Hicks, P. S., Escudero, K. W., Andrews, C. L., McSwiggen, J. A., & von Hippel, P. H. (1988) *J. Mol. Biol. 199*, 623–636.

Bloomfield, V., Dalton, W. O., & van Holde, K. E. (1967) *Biopolymers 5*, 135.

Brennan, C. A., Dombroski, A. J., & Platt, T. (1987) *Cell 48*, 945–952.

Chen. R. F., & Scott, C. H. (1985) *Anal. Lett. 18*, 393–421.

Davies, G. E., & Stark, G. R. (1970) *Proc. Natl. Acad. Sci. U.S.A. 66*, 651–656.

Dolan, J. W., Marshall, N. F., & Richardson, J. P. (1990) *J. Biol. Chem. 265*, 5747–5754.

Dombrowski, A. J., & Platt, T. (1988) *Proc. Natl. Acad. Sci. U.S.A. 85*, 2538–2542.

Engel, D., & Richardson, J. P. (1984) *Nucleic Acids Res. 12*, 7389–7400.

Epe, B., Wooley, P., Steinhauser, K. G., & Littlechild, J. (1982) *Eur. J. Biochem. 129*, 211–219.

Fairclough, R., & Cantor, C. (1972) *Methods Enzymol. 48*, 347–379.

Finger, L. R., & Richardson, J. P. (1981) *Biochemistry 20*, 1640–1645.

Finger, L. R., & Richardson, J. P. (1982) *J. Mol. Biol. 156*, 203–219.

Förster, W. (1948) *Ann. Phys. (Leipzig) 2*, 55.

Geiselmann, J., Yager, T. D., Gill, S. C., Calmettes, P., & von Hippel, P. H. (1992) *Biochemistry* (preceding paper in this issue).

Gogol, E. P., Seifried, S. E., & von Hippel, P. H. (1991) *J. Mol. Biol. 221*, 1127–1138.

Hammes, B. D., & Rickwood, D. (1981) *Gel Electrophoresis of Proteins*, IRL Press, Oxford.

Klotz, I. M., Darnall, D. W., & Langerman, N. R. (1975) in *The Proteins* (Neurath, H., & Hill, R. L., Eds.) 3rd ed. pp 293–411, Academic Press, New York.

Lakowicz, J. R. (1983) *Principles of Fluorescence Spectroscopy*, Plenum Press, New York.

McSwiggen, J. A., Bear, D. G., & von Hippel, P. H. (1988) *J. Mol. Biol. 199*, 609–622.

Matthews, B. M., & Barnhard, S. A. (1973) *Annu. Rev. Biophys. Bioeng. 2*, 257–317.

Oda, T., & Takanami, M. (1972) *J. Mol. Biol. 71*, 799–802.

Platt, T., Brennan, C. A., Dombroski, A. J., & Spear, P. (1989) in *Molecular Biology of RNA*, pp 325–334, A. R. Liss, Inc., New York.

Pesce, A. J., Rosen, C. G., & Pasby, T. L. (1971) *Fluorescence Spectroscopy*, Marcel Dekker, New York.

Reynolds, J. A., & Tanford, C. (1970) *J. Biol. Chem. 245*, 5161–5165.

Richardson, J. A., & Rutschouser, C. E. (1986) *J. Mol. Biol. 189*, 413–419.

Ruggiero, A., & Hudson, B. (1989) *Biophys. J. 55*, 1111–1124.

Seifried, S. E., Wang, Y., & von Hippel, P. H. (1988) *J. Biol. Chem. 263*, 13511–13514.

Seifried, S. E., Bjornson, K. P., & von Hippel, P. H. (1991) *J. Mol. Biol. 221*, 1139–1151.

Steiner, R. F. (1983) *Excited States of Biopolymers*, Plenum Press, New York.

Stitt, B. (1988) *J. Biol. Chem. 263*, 11130–11137.

Van Holde, K. E. (1975) in *The Proteins* (Neurath, H., & Hill, R. L., Eds.) 3rd ed., 225–291, Academic Press, New York.

Weber, G. (1954) *Trans. Faraday Soc. 50*, 552.